A Spine X-ray Image Retrieval System using Partial Shape Matching

Xiaoqian Xu, Dah-Jye Lee, Senior Member, IEEE, Sameer Antani, Member, IEEE, and L. Rodney Long, Member, IEEE

***Abstract*— In recent years, there has been a rapid increase in the size and number of medical image collections. Thus, development of appropriate methods for medical information retrieval is especially important. In a large collection of spine X-ray images, maintained by the National Library of Medicine, vertebral boundary shape has been determined to be relevant to pathology of interest. This paper presents an innovative partial shape matching (PSM) technique using dynamic programming (DP) for retrieval of spine X-ray images. The improved version of this technique called corner-guided DP is introduced. It uses 9 landmark boundary points for DP search and improves matching speed by approximately 10 times compared to traditional DP. The retrieval accuracy and processing speed of the retrieval system based on the new corner-guided PSM method are evaluated and included in this paper.**

***Index Terms*— Corner-guided, dynamic programming, image retrieval, partial shape matching, NHANES II**

I. Introduction

THERE has been growing interest in content-based indexing of biomedical images, especially for developing an automated or computer-aided interactive medical information retrieval system. A digital archive of 17,000 cervical and lumbar spine X-ray images from the second National Health and Nutrition Examination Survey (NHANES II) is maintained by the Lister Hill National Center of Biomedical Communications at National Library of Medicine (NLM) at the National Institutes of Health (NIH). An interactive retrieval system for these X-ray images is important for research purposes including finding pathological exhibits in a large survey collection, and education purposes including training medical students, etc. Another very important application is to provide reference to radiologists to assist diagnosis. Research work has been done to index and retrieve these images. We have developed query-by-sketch and query-by-example based methods for shape-based image retrieval, which offers visual search of these images. Development of a more powerful and user-friendly system is an ongoing project at NLM. The latest revision of this system supports hybrid image and text queries [1]-[2].

Content-Based Image Retrieval (CBIR) remains an active research area seeking representation methods and retrieval algorithms for color, shape, and texture. Fig.1 shows a spine X-ray image with the segmented shape contour. As shown, spine X-ray images generally have low contrast and poor image quality. In these images no meaningful texture information exists. Shape, however, effectively describes various pathologies identified by medical experts as being consistently and reliably found in this image collection. About 4500 cervical and lumbar shapes have been segmented from over 900 images in the collection using an active contour based algorithm that uses orthogonal curves [3]. Despite the automated nature of the segmentation algorithm, manual intervention was occasionally necessary due to poor image quality.

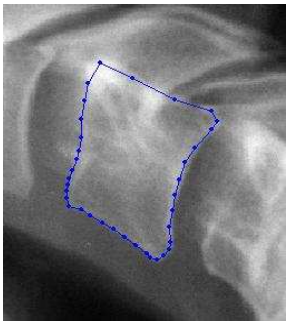

Fig. 1. X-ray image with the superimposed blue (or dark dotted line in black and white) shape contour. Shape contour has been proven to be the best feature to use.

Shape matching is a well-explored research area with many shape representation and similarity measurement techniques found in the literature [4]–[15]. Shape representation methods include Fourier descriptors [4]–[6], polygonal approximation [7], invariant moments [8]-[9], B-splines [10]–[11], deformable templates [12], and Curvature Scale Space (CSS) [13]–[14]. Most of these techniques were developed for whole shape matching, i.e., closed planar curve matching. The CSS shape representation method has been selected for MPEG-7

Manuscript received on March 12, 2005 and revised on February 22, 2006 and February 19, 2007. This work was supported by the National Library of Medicine under contract # 467-MZ301975.

X. Q. Xu was with the Department of Electrical and Computer Engineering, Brigham Young University, Provo, UT 84602 USA. She is now with KLA-Tencor Corporation, 160 Rio Robles, San Jose, CA 95134 USA (email: xiaoqian.xu@gmail.com)

D. J. Lee is with the Department of Electrical and Computer Engineering, Brigham Young University, Provo, UT 84602 USA (phone: 801-422-5923; fax: 801-422-0201; e-mail: djlee@ee.byu.edu)

S. K. Antani and L. R. Long are with the Lister Hill National Center for Biomedical Communications, National Library of Medicine, National Institutes of Health, Bethesda, MD 20894, USA (email: santani@mail.nih.gov rlong@mail.nih.gov)

standardization [13]–[14], [16]. However, based on the curvature zero-crossing, the CSS method is more suitable for shapes with distinct curvature variations such as leaf shapes than for smooth shapes with subtle curvature variations. Fourier descriptor has proven to be more efficient and robust than CSS in a review of shape representation and description techniques [15]. But as mentioned in [15], Fourier descriptor was not suitable for partial shape matching.

Our previous research work focused on whole shape matching for spine shapes [17]–[19]. Several different methods including Fourier descriptors, polygonal approximation, geometric global shape properties (such as eccentricity, elongation, etc), and invariant moments were implemented and evaluated for spine X-ray retrieval. However, whole shape matching techniques provided relatively low retrieval accuracy in retrieving similar pathological spine shapes.

For spine shapes, pathologies found on the spine X-ray images that are of interest to the medical researchers are generally expressed along the vertebral boundary. These pathologies include anterior osteophytes (AO), intervertebral disc degeneration and resulting disc space narrowing, subluxation and spondylolisthesis. Among them, work presented in this paper focuses on AOs that show up on the two anterior "corners" in the sagittal view and the deformation appears as a protrusion, as shown in Fig. 2.

In terms of AO pathology, therefore, there are critical intervals along the vertebral boundary that the radiologist would focus on rather than the whole shape. This indicates the main drawback of whole shape matching: *certain parts on the vertebra shape that are not of pathological interest may obscure the differences between critical regions and thus hinder accurate retrieval*.

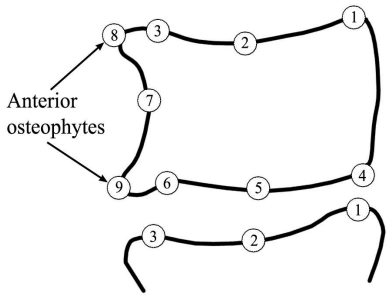

Fig. 2. Radiologist marked 9-point model for vertebral shape description. Points 8 and 9, if not coincident with Points 3 and 6, respectively, indicate the existence of osteophytes.

Partial shape matching (PSM) was investigated as an alternative to whole shape matching and to enable retrieval specific to the pathology on the anatomy of interest. In general, there is very little information in the literature on the application of partial shape matching for retrieval of medical images. It allows querying on some specific intervals along the vertebral boundary shape and searches for the best matching intervals on other whole shapes. This PSM concept theoretically addresses the same problem as *region*-based image retrieval which divides the whole image into several regions and weighs regions on their significance [20]–[21].

PSM also provides a way to deal with occlusion and distortion when comparing two incomplete shapes or distorted shapes [22]-[26]. Different shape representations such as wedge wave, inflection points, and line segments were used. The recent contribution by Petrakis et al [25] presented an approach for open shape matching using DP. Inflection points served as inputs to the shape representation method. The extracted shape features included the length, the area, and the rotation angle. DP selects the most promising candidate points to merge in its search for the match path with the least cost (highest similarity). Allowing merging points made this approach capable of addressing the matching problems in the presence of occlusion and distortion. However, inflection points are not suitable for rectangular spine shapes since a rectangular shape does not have a significant number of inflection points. Gdalyahu et al constructed a syntactic shape representation, whose primitives were line segments and whose attributes were length and absolute orientation [24]. The search was also achieved by using DP.

Arica et al introduced a perceptual shape descriptor [26]. Each point on the boundary was represented by the moments of the angles, each of which was formed by a pair of the bearings at a boundary point. The limitation of this method is that it requires uniformly-distributed shape data points. Shape data points for our application are not equally distributed because dense data points are needed to better describe the pathological details of the region of interest, e.g., the anterior osteophyte regions shown in Fig. 2. In other words, the anterior osteophyte regions need to be represented with more data points than other regions on a spine shape.

More often, shapes are represented by different numbers of points, different data point distributions or data sample spacing, which is the case for the spine shapes in our database. Also, noise may occur during the process of contour segmentation. Thus, the capability of merging data points that DP possesses is preferred.

Based on the perceptual shape descriptor in [26], we developed a multiple open triangle shape representation method, which does not require equally-distributed shape data points. A line segment method with two old attributes (length and absolute orientation) [24] and one new attribute (relative orientation) was also implemented for comparison. DP was implemented for both shape representations as our initial PSM work [27].

A high computational requirement is a significant drawback of DP, especially for a large medical image database. Based on the rectangular nature of spine shapes and the 9 point landmark model, corner-guided PSM using DP is proposed and presented in this paper. Limiting the possible search regions to four corners dramatically increases the search speed. An innovative approach has been taken to modify the traditional DP to perform matching starting from a corner, which is a point in the middle of the whole matching segment, rather than the first point of the matching segment.

In this paper we will start Section II with an introduction of the 9-point landmark model that radiologists use to describe vertebral shapes. We will then introduce our algorithm capable of automatically locating the 9-point model. Section III will focus on PSM and the improved corner-guided PSM using the modified DP. The retrieval system based on PSM as well as the retrieval performance evaluation will be discussed in Section IV. Our conclusions will appear in Section V.

I. 9-point Model

Fig. 2 shows a 9 morphometric landmark-point model schematic. Points 8 and 9 indicate the existence of AO. For normal vertebrae, points 8 and 9 will coincide with points 3 and 6, respectively. The 9-point model helps radiologists and bone morphometrists in marking relevant pathology on spine X-ray images. The semantic relevance of the 9 points in the sagittal view is as follows:

1) Points 1 and 4 mark the upper and lower posterior "corners" of the vertebra, respectively.
2) Points 3 and 6 mark the upper and lower anterior "corners" of the vertebra, respectively.
3) Points 2 and 5 are the median along the upper and lower vertebra edge.
4) Point 7 is the median along the anterior vertical edge of the vertebra.
5) Points 8 and 9 indicate the presence of the upper and lower anterior osteophytes respectively. These points are typically marked at the osteophyte extremities.

We have developed an algorithm for automatic localization of these points by applying heuristics based on their semantic relevance [28]. This auto-localization algorithm provides the corner information for our proposed corner-guided PSM using DP and thus is an essential part of the retrieval system. The corner detection part of the 9-point localization algorithm is included as follows and more details can be found in our earlier paper [28].

Curve evolution technique [29]-[30] was implemented to reduce the number of data points while keeping the most significant ones. This is achieved by iteratively comparing a relevance measure expressed in Equation (1) of all remaining vertices on the shape.

$$K(s_1,s_2)=\frac{|(\beta(s_1,s_2)-180)|\,l(s_1)l(s_2)}{l(s_1)+l(s_2)} \qquad (1)$$

where $\beta(s_1,s_2)$ is the angle between two adjacent line segments s_1 and s_2, and $l(s_1)$ and $l(s_2)$ represent the normalized length (to the total length of the whole shape) of s_1 and s_2, respectively. Higher relevance value means that the vertex has larger contribution to the shape of the curve. The angle $\beta(s_1,s_2)$ was calculated as the outer angle between two line segments. The curve evolution stopped when the number of remaining vertices was down to 20. The bend angle as illustrated in Fig. 3 was then calculated for each of those 20 points and it was calculated in a way so that the clockwise turn gives a negative angle whereas a counter clockwise turn gives a positive angle. Thus, only the vertices with a positive bend angle can be a corner. The corners were detected according to the following rules:

1. Vertices with a negative angle will be removed.
2. If there are two adjacent vertices and both with a positive bend angle, the vertex with the smaller bend angle will be removed.
3. If there are more than 4 points left, sequentially connect all remaining vertices, recalculate their bend angles, and then repeat steps 1 and 2.

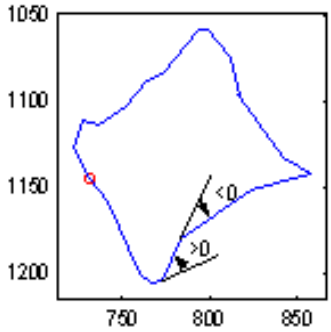

Fig. 3. Bend angle

The auto-localization algorithm has been tested on a subset of 250 vertebral shapes from those marked by a board certified radiologist. An evaluation was done by comparing automatic localization results with expert marked points. As shown in Fig. 1, spine contours in X-rays typically have a broad edge. This inevitably induces the slight difference between the visual contours on the images and the segmented spine shapes even though the segmented shapes well retain the spine silhouettes. Fig. 4 shows two samples of the 9-point auto-localization algorithm's performance with one 7-point (without AO) and one 9-point (with AO). The crosses represent the points marked by the radiologist on the X-ray images and the circles represent the points localized by the algorithm on the spine shapes. As we have mentioned about the possible edge shift caused by the broad edge, the two sets of 9-points are not identical. However, the algorithm performs fairly well in detecting the AOs and the corners. The minimum L_2 distance between the two sets of 9 points was calculated to evaluate the accuracy of the algorithm. For 93% of the 250 tested shapes, the minimum distance was below 20 pixels, which we consider to be very impressive.

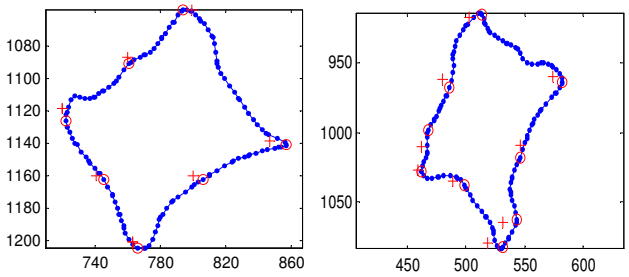

Fig. 4. Auto-localization of 9-point model. The crosses represent the expert marked points and the circles represent the points our algorithm detected.

II. Partial Shape Matching

A. Shape Representation Methods

1) Line Segments

A line segment is formed by connecting two adjacent points on the shape contour. Suppose a shape has N points: if it is closed, it has N line segments; if it is open, it has $N-1$ line segments. Besides the two shape features (length and absolute orientation) used in [24], relative orientation is proposed as the third feature. They are described as follows:

-- Length: 2-norm of the line segment.

-- Absolute Orientation: The angle between the abscissa axis and the line segment, which has the same length as the original line segment but starting from the original point.

-- Relative Orientation: Bend angle between two adjacent line segments.

Based on these shape features, we can define the similarity between two line segments a_k and $a_l^{'}$. We denote the features of a_k, $a_l^{'}$ -- absolute orientation and length -- by (θ, l) and $(\theta^{'}, l^{'})$, respectively. The reference feature vectors are calculated for both the query and the object shape: (θ_0, l_0) and $(\theta_0^{'}, l_0^{'})$, which are the mean of both features of all the line segments on either query or the object shape. In order to obtain the scale-invariant length similarity measurement, the global alignment, which is the overall average scale ratio between the query and the object shape, will be calculated and denoted as $c_0 = l_0 / l_0^{'}$. Then with $c = l / l^{'}$, the length similarity can be expressed as:

$$S_l(l, l^{'} \mid l_0, l_0^{'}) = \frac{4cc_0 + (c^2 - 1)(c_0^2 - 1)}{(c^2 + 1)(c_0^2 + 1)} \tag{2}$$

, which calculates the difference between the overall scale factor and an individual scale factor as the distance in terms of length [24].

The absolute orientation similarity is:

$$S_\theta(\theta, \theta^{'} \mid \theta_0, \theta_0^{'}) = \cos[(\theta - \theta^{'}) - (\theta_0 - \theta_0^{'})] \tag{3}$$

The relative orientation similarity is:

$$S_{rel} = \cos(\theta_{rel} - \theta_{rel}^{'}) \tag{4}$$

During the DP search process, the cost is used instead. For each shape feature above, the cost is calculated as *1.0-similarity*. This similarity/cost relationship is applied to the multiple open triangle shape representation method as well and is described in the next section. The costs for each feature are denoted as C_l, C_θ, and C_{rel}. Thus the total cost is defined as the summation of the three:

$$C = C_l + C_\theta + C_{rel} \tag{5}$$

2) Multiple Open Triangles

An open shape can be expressed as $M = M_1, M_2, M_3, ..., M_N$, where M_i is the i^{th} point on the shape with the coordinate (x_i, y_i). From the second point on, each point has at least one previous point and one subsequent point. An open triangle is formed by connecting the previous point to the current point and the current point to the subsequent point. For those points which have more than one previous point, another open triangle is formed by connecting M_{i-2} to M_i and M_i to M_{i+2}. Therefore, each data point can be represented by multiple open triangles as shown in Fig. 5. In our application, we set $K = 3$ as the largest number of such open triangles associated with one point.

As shown in Fig. 5, point M_2 only has one open triangle; point M_6 could have up to 5 open triangles, but only the first three open triangles as shown in the figure are used to represent this point. The angle θ associated with an open triangle is also illustrated in Fig. 5. The angle is actually the supplementary angle of the relative orientation we calculated for the line segments. The lengths of the two sides of an open triangle are also calculated as the features and the length similarity is calculated in the same way as for the line segment representation method. The overall angle similarity for each data point is calculated as:

$$S_\theta = \frac{1}{n}\sum_{i=1}^{i=n} \cos(\theta_i - \theta_i^{'}) \tag{6}$$

, where n is the number of the open triangles. For example, when using three open triangles to represent one data point, the overall angle similarity is the average of the three individual angle similarities (one for each open triangle).

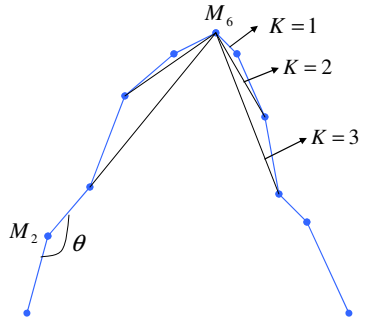

Fig. 5. Multiple open triangles of a partial shape with 11 data points. There is only one open triangle associated with M_2. There are possibly 5 open triangles associated with M_6. Each open triangle can be measured by the average length of the two line segments and the angle between them.

B. Traditional Dynamic Programming

DP is a powerful tool for finding a desired path through all the possible paths. In partial shape matching, DP finds the best matching path with the minimum cost. Spine shapes in our database have different number of points and different point distributions. DP is desired because of its capability of merging data points.

Traditional DP searching strategy is explained as follows. Suppose there is an open shape query A consisting of 5 points, and an object shape B which is a closed shape consisting of 7 points. In searching for the match of query A to shape B, the algorithm builds a DP table (Table I), where rows and columns correspond to the points of A and B, respectively [25]. The number of columns of the DP table is twice the number of

points on B , which ensures that every point on B could be a starting matching point for a complete match by having subsequent points. DP search starts from the cells (marked as S in Table I) at the bottom row which is denoted as the 'Initialization Area' and proceeds upward and to the right. Each cell of the table contains the previous matching node location and the total cost associated with the matching path up to this current cell. After filling out the top row which is the 'Termination Area' (marked as T in Table I), all the possible matches of shape B to query A have been explored and are able to trace back starting from the termination area. The matching path with the minimum cost is finally picked to give the best match.

TABLE 1
A SEARCHING TABLE FOR TRADITIONAL DP

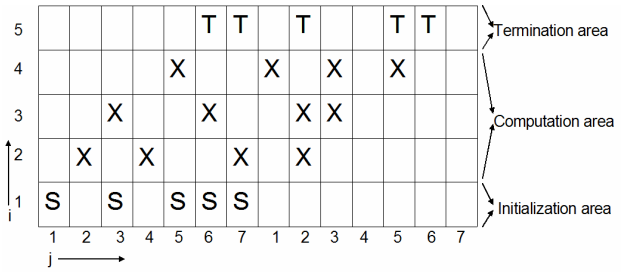

During the process of filling the DP table, merging of the data points occurs if a lower cost can be obtained. For example, if the cost of matching points 2 and 3 on query A with points 4 and 6 on shape B , respectively is smaller than the cost of matching points 2 and 3 on query A with points 4 and 5 on shape B , DP algorithm will choose to merge point 5 on shape B to achieve a lower cost.

The total cost includes the cost contributed by the corresponding shape features and a merging cost if any merging occurs. The merging cost serves as the penalty for removing a point that is actually on the shape since it is not guaranteed to be noise. The merging cost is measured as the *sine* value of its bend angle or relative orientation, which reflects the significance of the merged point. When more than one point is merged, the total merging cost is the sum of the merging cost associated with each merged point as shown in Equation (7):

$$C_{mer} = \sin(\theta_{rel1} + \theta_{rel2} + \theta_{rel3} + ...) \quad (7)$$

For instance, as shown in Fig. 6, suppose there are four points and the matching path is from point 1 directly to point 4, which means point 2 and 3 are removed. Then the merging cost associated with this matching path is computed as $C_{mer} = \sin(\theta_{rel2} + \theta_{rel3})$.

Traditional DP has been implemented for both line segment and multiple open triangle shape representations and has been tested on 15 shapes with around 100 points on each shape [27]. The results showed that multiple open triangle representation performed better than line segment representation, which accords with the fact that multiple open triangle method provides more information about the contribution and the importance of a point to the curve. DP is very computationally expensive and sensitive to noise. Therefore, for reasons of efficiency, a limit was set on the maximum number of consecutively merged points. However, even with this limitation, DP still turned out to be a long process by trying every point on the object shape as a possible starting matching point. Approximately one minute was required to find the best matching path for one shape with around 100 points. This made it impractical to integrate the algorithm for online search of a large medical image database.

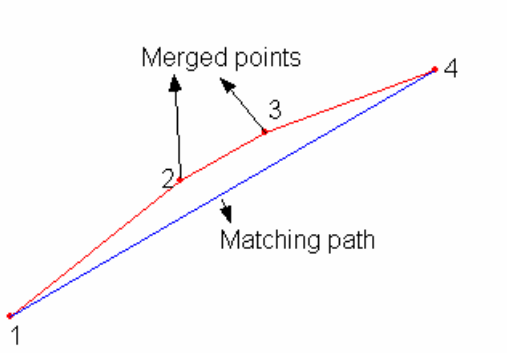

Fig. 6. Merging process. The merging cost associated with each merged point is measured in Equation (7). The new line segment is formed as a straight line connecting points 1 & 4 if points 2 & 3 are merged (removed).

C. *Corner- Guided DP*

As we have addressed in Section II, the vertebrae shapes tend to be rectangular with 9 critical landmark points that help indicate pathology. Partial shape matching allows querying on any part that the user is interested in. Since pertinent pathology (AO) occurs at the "corners", we can use PSM at this interval for retrieval.

The localized 9-piont on vertebral boundaries are stored in a database for run time use. Storing these data in the database helps to speed up corner-guided DP search.

Traditional DP needs to be modified when guided by the corners. As a first step, the "corners" on the query shape are aligned with those on the target shape. This limits the similarity search to the boundary segment at the corners. Thus, for a whole vertebral shape with four corners, four potential partial matching segments will be identified such that each contains one corner. Among these four matching segments, one with least cost is selected as the most similar matching part on the current object shape.

Because of the better performance, multiple open triangles were chosen to represent the shapes for corner-guided DP. Table II illustrates corner-guided DP, which still has the same layout as the traditional DP table except for two termination areas. Suppose the query A has 7 points and the object shape B has 9 points. Instead of starting from Initialization area in Table I, corner-guided DP first matches the corners as indicated as ' C ' in Table II on both the query and the object shape, which is actually a point in the Computation area in Table I. Starting from ' C ', DP search is performed in both directions simultaneously and independently until reaching the termination areas. At each cell, the total cost is computed as in

Equation (8), and compared with the previous lowest cost to determine which path to keep.

$$C_{total} = W_1 \times C_l + W_2 \times C_\theta + W_3 \times C_{mer} \quad (8)$$

W_i is the adjustable weight for the cost of each feature.

TABLE II
CORNER-GUIDED DP SEARCHING TABLE

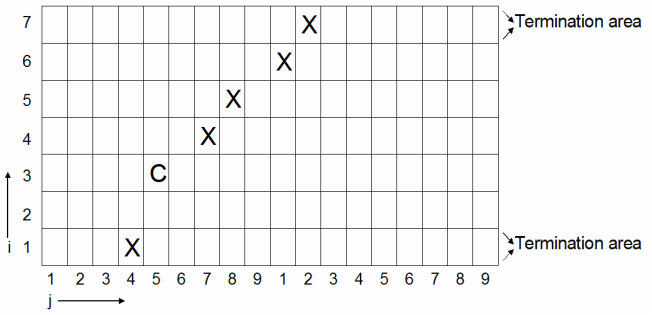

The outline of the corner-guided DP search for one corner is described as follows:

1) Search for one line segment on both sides of the targeted corner, which forms an open triangle. Calculate the cost of each individual possible matching path and get the first best matched open triangle with the lowest cost. For example in Table II, point 4 and 7 on shape *B* are chosen to be the best match to point 1 and 4 on query *A* , respectively.
2) If one side reaches the termination area first, go to step 4; otherwise, search for the next one line segment on both sides. The new cost part is produced by matching the second open triangle of the corner and the first open triangle of the two points selected in Step 1.
3) If one side hits the termination area first, go to step 4; otherwise, search for the next one line segment on both sides. The new cost part is produced by matching the third open triangle of the corner, the second open triangle of the two points selected in Step 1, and the first open triangle of both points selected in Step 2. Since the maximum number of open triangles associated with one point is limited to 3, this step completes the matching of all possible three open triangles associated with the corner.
4) Take each side of the corner and continue the matching according to the traditional DP. Each side stops independently when it reaches the termination area. The whole matching finishes when both sides reach the corresponding termination area.

Corner-guided DP only selects four best matching paths for one individual object shape. However, the traditional DP selects a best matching path for every point on the object shape. Even though the time of completing a best matching path varies from point to point, the assumption that the time is equal can be made statistically. Thus, suppose an object shape has N points, the corner-guided DP will be N/4 times faster than the typical DP. So the more points the object shape has, the more efficient the corner-guided DP is compared to the traditional DP. This is a significant improvement especially when retrieving images from a large database.

III. System, Performance, and Evaluation

Fig. 7 shows the user interface of the retrieval system implemented in Matlab. "Load Query" allows the user to select a spine shape from the database, which is shown in blue (solid line). "PSM Select" allows the user to specify a specific region of interest on the whole shape, which is then highlighted in red (solid line with dots). The system provides two retrieval methods: corner-guided Procrustes [31] distance and corner-guided PSM with DP using multiple open triangle representation. The Procrustes method performs a linear transformation (translation, rotation, and scaling) on one shape to find the best match between two shapes. Suppose (x, y) and (x', y') are n boundary point coordinates of shapes of A and B, respectively. The Procrustes distance is then represented by Equation (9), where shape A is translated by (T_x, T_y), scaled by S, and rotated by θ:

$$P = \sum_{i=1}^{n} \left\| \begin{bmatrix} S\cdot\cos\alpha & -\sin\alpha & T_x \\ \sin\alpha & S\cdot\cos\alpha & T_y \\ 0 & 0 & 1 \end{bmatrix} \begin{bmatrix} x_i \\ y_i \\ 1 \end{bmatrix}_A - \begin{bmatrix} x_i' \\ y_i' \\ 1 \end{bmatrix}_B \right\|^2 \quad (9)$$

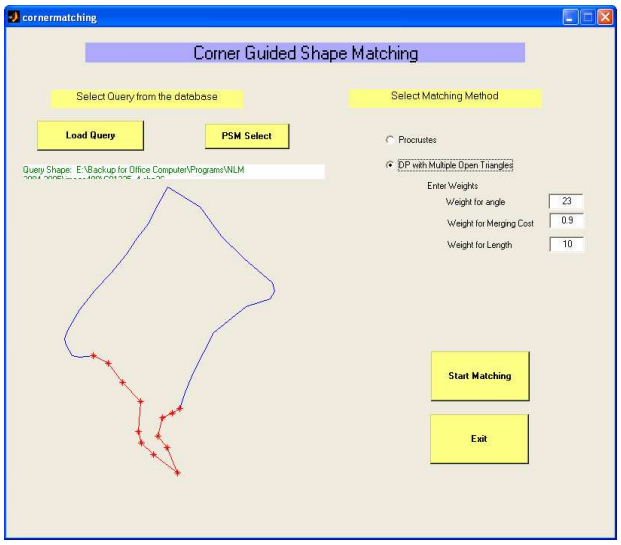

Fig. 7. System user interface. Users are allowed to select a query shape from the database and to highlight the partial shape as the region of interest.

The drawback of the Procrustes distance measure is that it requires the same number of points on the two partial/whole shapes. For corner-guided PSM method, the system provides a set of default values for the weights shown in Equation (8) and also the option for the user to specify different weights if so desired. A set of 801 cervical shapes and 972 lumbar shapes segmented from a total of 400 images have been chosen for performance evaluation. We used two interior corners of each of these 1773 shapes for study. These 3546 corners were classified as having server, moderate, or slight/normal AO pathology. Approximately 23.54% of these corners were considered with AO pathology (server or moderate). The rest of them were considered non-pathological. Ten queries (five cervical and five lumbar) were chosen and the best 15 matches

to each query were retrieved for study. Human relevance judgments were employed to evaluate the effectiveness of the two methods. Specifically, three human reviewers inspected the retrieval results of a query and judged whether it was a similar match to the query.

Fig. 8 shows the retrieval results of a partial query using corner-guided PSM, while Fig. 9 gives the retrieval results of the same query using corner-guided Procrustes distance. As shown, corner-guided PSM performs better in detecting the details of the angle changes of the query. Since DP performs shape matching based on multiple open triangles, it extends the matching path line segment by line segment. Procrustes treats the partial query as a "whole shape" and performs the alignments globally to find the minimum distance. Thus, theoretically DP is superior to Procrustes in detecting the details. Furthermore, DP allows merging data point and does not require the same number of points to match two partial shapes. This also enables DP to overcome noise on the contour by merging/removing noisy data points. Procrustes distance requires the same number of points to match two shapes and thus cannot deal with noise or different point distributions. Fig. 10 shows the retrieval results of another query using corner-guided PSM.

A simplified and common way of computing Precision and Recall was used to give a statistical evaluation of the corner-guided PSM method, corner-guided Procrustes distance, and the traditional DP method:

1) Precision is the percentage of qualifying shapes retrieved with respect to the total number of retrieved shapes.
2) Recall is the percentage of qualifying shapes retrieved with respect to the total number of similar shapes in the database.

Because of the subjective nature of human vision, human relevance was used to provide the ground truth in most shape retrieval result evaluations [25]. Three human subjects contributed their judgment to the evaluation of this spine X-ray retrieval system. Due to the large volume of the database, it is very difficult to find all the similar shapes manually in the database for a specific query. Matches for all 10 queries from half of the entire database were picked by human judges and the assumption that there is equal number of similar shapes to a specific query in both halves of the database was made.

The precision-recall results are plotted in Fig. 11. The horizontal axis corresponds to the measured recall while the vertical axis corresponds to precision. The plot contains 15

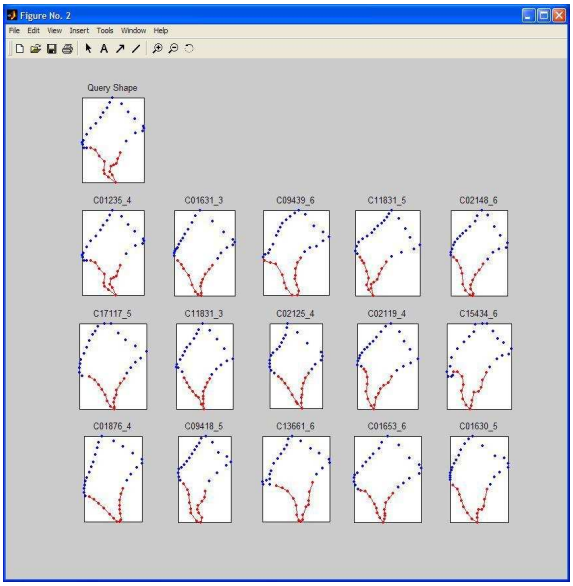

Fig. 9. Matching results using corner-guided Procrustes distance measure. The system retrieved 15 similar shapes from the database using the same query shape as the one shown in Fig. 8. Based on human judgment and comparing with other shapes in the database, the system incorrectly retrieved at least four shapes. The obvious errors are retrievals #3 and #11.

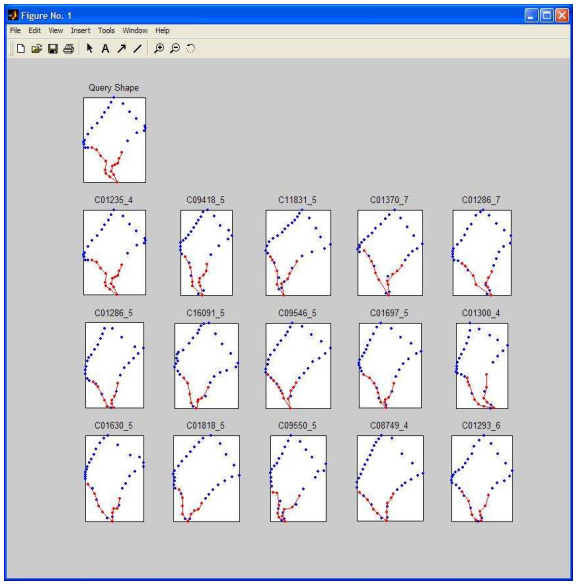

Fig. 8. Matching results using corner-guided PSM. The system retrieved 15 similar shapes from the database. Based on human judgment and comparing with other shapes in the database, the system successfully retrieved the top 15 similar shapes.

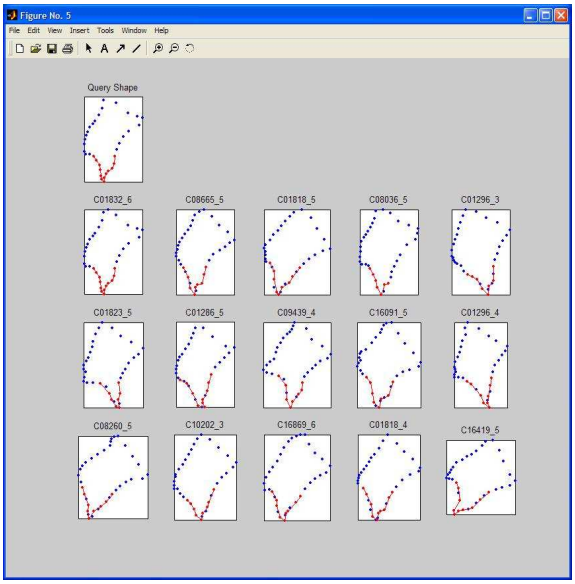

Fig. 10. Matching results of a different query using corner-guided DP. The system retrieved 15 similar shapes from the database. Based on human judgment and comparing with other shapes in the database, the system successfully retrieved the top 15 similar shapes. The retrieval result seems to be slightly better than the one shown in Fig. 8.

points, which corresponds to 15 best matches and each point in the plot is the average of 10 queries. The first point from the left of the plot corresponds to the average precision and recall values for the best match of the 10 queries, while the second point from the left corresponds to the average precision and recall values for the top 2 matches, and so on. Higher precision and higher recall represent better retrieval performance. The precision of the proposed corner-guided PSM using DP starts from 100% (successfully retrieves the top match for all 10 queries) and drops down gradually as a larger number of matches is considered. For the 10 queries we picked, the lowest precision of corner-guided PSM is still above 85%. And corner-guided PSM has a consistently higher precision than corner-guided Procrustes distance. Traditional DP, on the other hand, presents a very comparable precision with corner-guided PSM.

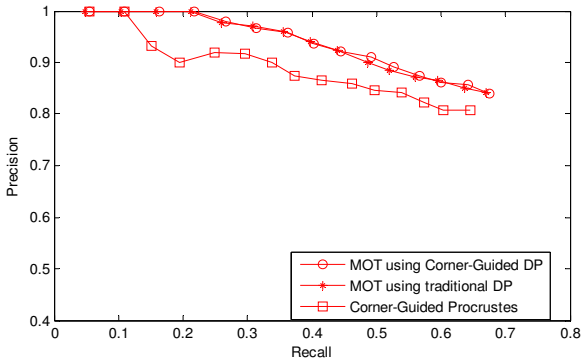

Fig. 11. Precision-Recall Results

The time efficiency of these three methods was also examined. First, 9 points of each shape in the database can be pre-calculated and stored. Therefore, the time for 9-point localization does not contribute to the following processing times. The average processing times for corner-guided PSM, corner-guided Procrustes, and traditional DP are 42 seconds, 19 seconds, and 400 seconds. Thus, compared to the traditional DP, corner-guided PSM using the modified DP speeds up the retrieval process by approximately 10 times. Although corner-guided PSM is slower than Procrustes, its average processing time is feasible for an image retrieval system.

IV. Conclusion

A spine X-ray image retrieval system has been described in this paper. According to the 9-point model and the shape nature of vertebral shapes, we introduced a corner-guided PSM method that uses a multiple open triangle shape representation method and a modified DP for matching. This method is invariant to translation, scaling, rotation, and the starting point selection. Tested on retrieving 15 best matches for 10 queries, this method has impressively high precision. With higher processing efficiency than the traditional DP approach, corner-guided PSM is a very promising and practical method for spine shape retrieval. The corner-guided PSM processing speed can be further improved if implemented with a more efficient programming language and development environment than Matlab. The weights of merging cost, length, and the angle are adjustable by the user during the retrieval process. However, the user usually does not have the knowledge of how different weights can change the retrieval results. Thus, our future work includes building an interactive retrieval environment to allow the user to provide relevance feedback [32] so as to automatically adjust the weights to refine the retrieval results. The sensitivity of the retrieval method on these weights can also be examined during the relevance feedback process.

V. Acknowledgment

This research was supported by the Intramural Research Program of the National Institutes of Health (NIH), National Library of Medicine (NLM), and Lister Hill National Center for Biomedical Communications (LHNCBC).

References

[1] L.R. Long, S. Antani, and G.R. Thoma, "Image informatics at a national research center", *Computerized Medical Imaging and Graphics*, vol. 29, Feb 2005, pp. 171-193.

[2] S. Antani, L.R. Long, and G.R. Thoma, "A Biomedical Information System for Combined Content-Based Retrieval of Spine X-ray Images and Associated Text Information", *The* 3rd *Indian Conference on Computer Vision, Graphics, and Image Processing (ICVGIP '02)*, India, Dec. 2002, pp. 242-47.

[3] Tagare HD, "Deformable 2-D template matching using orthogonal curves", *IEEE Trans. Med Imaging,* vol. 16, issue 1, Feb. 1997, pp. 108-117.

[4] C. Zahn and R. Roskie, "Fourier descriptors for plane closed curves", *IEEE Computer* C-21(3), pp. 269 – 281, 1972.

[5] T.D. Bui, G.Y. Chen, and L. Feng, "An orthonormal-shell-fourier descriptor for rapid matching of patterns in image database", *Internationl Journal of Pattern Recognition and Artificial Interlligence,* vol. 15, no. 8, pp. 1213 – 1229, 2001.

[6] Z. Ping, Y. Sheng, S. Deschenes, and H. Arsenault, "Fourier-Mellin descriptor and interpolated feature space trajectories for 3-D object recognition", *Optical Engineering,* vol. 39, no. 5, pp. 1260 – 1266, 2000.

[7] L. J. Latecki and R. Lakämper, "Shape description and search for similar objects in image databases", State-of-the-Art in Content-Based Image and Video Retrieval, R. C. Veltkamp, H. Burkhardt and H. P. Kriegel, eds., Computational Imaging and Vision 22, pp. 69 – 96, Kluwer Academic Publishers, 2001.

[8] M. K. Hu, "Visual pattern recognition by moment invariants", *IRE Transactions on Information Theory 8*, pp. 179 – 187, 1962.

[9] J. P. Eakins, J. D. Edwards, J. Riley and P. L. Rosin, "A comparison of the effectiveness of alternative feature sets in shape retrieval of multi-component images", *SPIE conference on Storage and Retrieval for Media Databases*, vol. 4315, pp. 196 – 207, 2001.

[10] C. de Boor, "On calculation with B-splines", *Journal of Approximation Theory,* vol. 6, pp. 50 – 62, 1972.

[11] F.S. Cohen, Zhaohui Huang, and Zhengwei Yang, "Invariant matching and identification of curves using b-splines curve representation", *IEEE Trans. Image Processing,* vol. 4, Jan. 1995, pp. 1 – 10.

[12] A. K. Jain, Y. Zhong and S. Lakshmanan, "Object matching using deformable templates", *IEEE Trans. Pattern Analysis and Machine Intelligence*, vol. 18, no. 3, pp. 267 – 278, 1996.

[13] Mokhtarian, F. and Mackworth, A.K., "A theory of multiscale, curvature-based shape representation for planar curves", *IEEE Trans. Pattern Analysis and Machine Intelligence,* vol. 14, Aug. 1992, pp. 789 – 805.

[14] F. Mokhtarian and S. Abbasi, "Matching shapes with self-intersections: applications to leaf classification", *IEEE Trans. Image Processing,* vol. 13, no. 5, May 2004, pp. 653 – 661.

[15] Dengsheng Zhang and Guojun Lu, "Review of shape representation and description techniques", *Pattern Recognition,* vol. 37, issue 1, Jan. 2004, pp. 1 – 19.

[16] M. Bober, "MPEG-7 visual shape descriptors", *IEEE Trans. Circuits and Systems for Video Technology,* vol. 11, no. 6, June 2001, pp. 716 – 719.
[17] S. Antani, L. R. Long, G. R. Thoma, and D. J. Lee, "Evaluation of Shape Indexing Methods for Content-based Retrieval of X-Ray Images", *SPIE Electronic Imaging, Storage and Retrieval for Media Databases*, vol. 5021, January 2003, pp. 405 – 416.
[18] D. J. Lee, S. Antani, and L. R. Long, "Similarity Measurement Using Polygon Curve Representation and Fourier Descriptors for Shape-based Vertebral Image Retrieval", *SPIE Medical Imaging, Image Processing*, vol. 5032, February 2003, pp. 1283 - 1291.
[19] S. Antani, L.R. Long, G.R. Thoma, and D.J. Lee, "Anatomical Shape Representation in Spine X-ray Image", in *Proceedings of IASTED International Conference on Visualization, Imaging and Image Processing*, Benalmadena, Spain, September 8-10, 2003, pp. 510-515.
[20] N. Vasconcelos and A. Lippman, "Bayesian representations and learning mechanisms for content-based image retrieval", *in Proceedings of SPIE: Storage and Retrieval for Media Databases,* vol. 3972, Jan. 2000, pp. 43 – 54.
[21] B. Moghaddam, H. Bierman, and D. Margaritis, "Defining image content with multiple regions-of-interest", in *Workshop in Content-based Access to Image and Video Libraries,* pp. 89 – 93, 1999, Fort Collins, Colorado.
[22] K. Mori, M. Ohira, M. Obata, K. Wada, and K. Toraichi, "A Partial Shape Matching Using Wedge Wave Feature Extraction", *1997 IEEE Pacific Rim Conference on Communications, Computers and Signal Processing – '10 Years PACRIM 1987 – 1997 – Networking the Pacific Rim'*, vol. 2, Aug. 1997, pp. 835 – 838.
[23] M. Werman and D. Weinshall, "Similarity and Affine Invariant Distances between 2D Point Sets", IEEE Transactions on Pattern Analysis and Machine Intelligence, Vol. 17, No. 8, Aug. 1995, pp. 810 – 814.
[24] Y. Gdalyahu and D. Weinshall, "Flexible Syntactic Matching of Curves and Its Application to Automatic Hierarchical Classification of Silhouettes", *IEEE Trans. Pattern Analysis and Machine Intelligence*, Vol. 21, No. 12, Dec. 1999, pp. 1312 – 1328.
[25] E. Petrakis, A. Diplaros, and E. Milios, "Matching and Retrieval of Distorted and Occluded Shapes Using Dynamic Programming", *IEEE Trans. Pattern Analysis and Machine Intelligence*, Vol. 24, No. 11, Nov. 2002, pp. 1501 – 1516.
[26] Nafiz Arica and Fatos T. Yarman Vural, "A Perceptual Shape Descriptor", in *Proc. of the 16th International Conference on Pattern Recognition*, Vol. 3, Aug. 2002, pp. 375 - 378.
[27] Xiaoqian Xu, D. J. Lee, S. Antani and L. R. Long, "Partial shape matching of spine X-ray shapes using dynamic programming", in *Proc. 17th IEEE Symposium on Computer-Based Medical Systems*, Bethesda, MD, June 24-25 2004, pp. 97 – 102.
[28] Xiaoqian Xu, D. J. Lee, S. Antani and L. R. Long, "Localizing Contour Points for Indexing an X-ray Image Retrieval System", in *Proc. 16th IEEE Symposium on Computer-Based Medical Systems*, New York, June 26-27, 2003, pp. 169 – 174.
[29] D. M. Wuescher and K. L. Boyer, "Robust contour decomposition using a constant curvature criterion", *IEEE Transactions on Pattern Analysis and Machine Intelligence*, vol. 13, no.1, Jan. 1991, pp. 41-51.
[30] A. K. Mackworth and F. Mokhtarian, "The renormalized curvature scale space and the evolution properties of planar curves", *Proceedings of IEEE Computer Society Conference on Computer Vision and Pattern Recognition*, Jun 1988, pp. 318-326.
[31] Dryden, IL and Mardian, KV, *Multivariate shape analysis,* London: John Wiley & Sons.
[32] Yong Rui, Huang, T.S., M. Ortega, and Mehrotra, S., "Relevance feedback: a power tool for interactive content based image retrieval", *IEEE Trans. Circuits and Systems for Video Technology*, vol. 8, Sept. 1998, pp. 644-655.

Xiaoqian Xu received her B.S. degree in electrical engineering from Najing University, China in 2002. She then received her Ph.D degree in electrical engineering from Brigham Young University, Provo, UT in December 2006.

During her Ph.D studies, she worked as a summer intern at the National Institutes of Health during the summers of 2003 and 2005. Her Ph.D research topics included Content-Based Image Retrieval, relevance feedback, and indexing with applications to medical image retrieval. She is currently working as an applications engineer at KLA-Tencor Corp. in San Jose, CA.

Dah-Jye Lee received his B.S.E.E. from National Taiwan University of Science and Technology in 1984, M.S. and Ph.D. degrees in electrical engineering from Texas Tech University in 1987 and 1990, respectively. He also received his MBA degree from Shenandoah University, Winchester, Virginia in 1999.

He is currently an Associate Professor in the Department of Electrical and Computer Engineering at Brigham Young University. He worked in the machine vision industry for eleven years prior to joining BYU in 2001. His research work focuses on Medical informatics and imaging, shape-based pattern recognition, hardware implementation of real-time 3-D vision algorithms and machine vision applications.

Dr. Lee is a senior member of IEEE and a member of SPIE. He has actively served the research community as a paper and proposal reviewer and conference organizer.

Sameer Antani received his B.E. (Computer) from University of Pune in 1994, M.E. and Ph.D. degrees in Computer Science and Engineering from the Pennsylvania State University in 1998 and 2001, respectively.

He is currently a Staff Scientist with the Lister Hill National Center for Biomedical Communications an intramural R&D division of the National Library of Medicine which is an institute within the U.S. National Institutes of Health. His research interests are in data management of and retrieval from, large biomedical multimedia archives. His research includes content-based indexing, and retrieval of biomedical images, combining image and text retrieval, and next-generation documents that are enriched with interconnections to data sets and multimedia content.

Dr. Antani is a member of IEEE and IEEE Computer Society. He serves on the steering committee for IEEE Symposium for Computer Based Medical Systems (CBMS). He is a reviewer for several journals including various IEEE transactions. .

L. Rodney Long received his B.A. and M.A. degrees in mathematics from the University of Texas in 1971 and 1976, respectively, and M.A. degree in applied mathematics from the University of Maryland in 1987.

Since 1990 he has been an Electronics Engineer in the Communications Engineering Branch of the National Library of Medicine. He previously worked for 14 years in industry as a programmer and engineer. His research work is concerned with Content-Based Image Retrieval, image processing, and image databases for biomedical applications.

He has been a member of IEEE since 1986 and has served as co-chair of the IEEE International Symposium of Computer-Based Medical Systems.